

## **SPECIALTY FIBERS DESIGNED BY PHOTONIC CRYSTALS**

**N. Nozhat and N. Granpayeh**

Faculty of Electrical Engineering  
K. N. Toosi University of Technology  
Tehran, Iran

**Abstract**—In this paper, several kinds of photonic crystal fibers (PCFs) have been proposed and characterized. Two types of PCF structures have been proposed, air holes in silica or silica rods in air in a triangular lattice around the core. It has been shown that by reshaping the cladding holes, varying the diameters of the holes in one or two rows around the core or changing the refractive index of the holes, different types of specialty fibers, such as dispersion shifted fibers (DSFs), non-zero dispersion shifted fibers (NZ-DSFs), dispersion flattened fibers (DFFs), dispersion compensating fibers (DCFs), and polarization maintaining fibers (PMFs), can be designed. The PCF core is silica to support the propagation of lightwave by total internal reflection (TIR) in the third telecommunication window. The chromatic dispersion, confinement loss and modal birefringence of the proposed specialty fibers have been numerically derived.

### **1. INTRODUCTION**

Photonic crystal fibers (PCFs) have attracted many researchers' attentions in recent years, because of their unique and remarkable properties compared to the conventional optical fibers [1]. Photonic crystal fibers are divided into two groups, named index guiding PCFs or holey fibers and photonic crystal band gap fibers. The index guiding PCFs have a silica core at the center of a structure consisting of multiple rows of air holes in silica with a triangular lattice, as cladding. The propagation of the lightwave in holey fibers, the same as conventional optical fibers, is by total internal reflection (TIR). In the other type of PCF a periodic structure consisting of holes in silica

---

Corresponding author: N. Granpayeh (granpayeh@eetd.kntu.ac.ir).

confine the lightwave with frequency in the structure photonic band gap (PBG) in a low-index core region [2, 3]. Photonic crystal fibers can be designed to show some noticeable properties, such as endlessly single mode operation, large effective core area, low or negative high chromatic dispersion, low confinement loss and high birefringence polarization maintaining fiber [4–14].

Control of chromatic dispersion in the PCFs is a very important issue for practical applications in dispersion compensation of optical communication systems and nonlinear optics. Design and analysis of some types of the PCFs, such as ultra-flattened chromatic dispersion [15–17], dispersion compensating fibers [18, 19] and polarization maintaining fibers have been reported [8, 20–23].

In this paper, in order to control the dispersion of PCFs to design different types of fibers, such as DSF, NZ-DSF, DFF, DCF and PMF, some new modifications have been proposed. For example, by introducing the air holes or rods with different refractive indices or holes with different radii, shifting the first row of the holes towards the core, replacing the circular holes of the cladding or core with elliptical ones and changing the refractive indices, the chromatic dispersion characteristics and the slope of the dispersion can be controlled.

In this paper, the effective refractive index and chromatic dispersion of different index guiding PCF structures have been derived by the finite difference time domain (FDTD). Various types of PCFs have been analyzed. Several specialty fibers designed by photonic crystal fibers have been proposed and their confinement loss and the modal birefringent characteristics have been obtained.

## 2. NUMERICAL ANALYSIS

There are various numerical methods for analyzing the PCFs, such as the plane wave expansion (PWE) method, the finite difference time domain (FDTD) method, the localized function method, the beam propagation method (BPM), the finite difference method (FDM) and the finite element method (FEM) [2, 24, 25]. Among various methods, FDTD is a general and powerful algorithm for calculating electromagnetic field distributions in the structures with arbitrary geometry. It is an accurate solution to Maxwell's equations and does not have any approximations or theoretical restrictions. Unlike the frequency domain method, it solves Maxwell's equations in time domain and we can get required information in broadband frequency domain by fast Fourier transform. PWE is also a good numerical method for calculating photonic band gap in periodic structures. Therefore, we have analyzed and modeled the PCF structures by the

FDTD and the PWE methods [26–32].

The chromatic dispersion of the PCFs can be determined by [1, 2, 5, 12]:

$$D = -\frac{\lambda}{c} \frac{d^2 n_{eff}}{d\lambda^2} + D_m \quad (1)$$

where the first term is the waveguide dispersion,  $\lambda$  and  $c$  are the wavelength and the speed of light in free space, respectively,  $n_{eff}$  is the effective refractive index of the PCF core and the second term is material dispersion. The mode effective refractive index can be obtained by  $n_{eff} = \beta/k_0$ , where  $k_0 = 2\pi/\lambda$  is the free space wave number and  $\beta$  is the longitudinal propagation constant along the fiber axis. The guided light has an effective index  $n_{eff}$  that satisfies the condition below [2]:

$$n_{FSM} < n_{eff} < n_{co} \quad (2)$$

where  $n_{co}$  is the core refractive index and  $n_{FSM}$  is the effective cladding refractive index corresponding to the fundamental space-filling mode.

To determine the waveguide dispersion, the effective refractive index of the structure must be derived as a function of  $\lambda/\Lambda$ , where  $\Lambda$  is the hole pitch. For deriving  $n_{eff}$  by the FDTD method [33], appropriate values for  $\Delta x$ ,  $\Delta y$ ,  $\Delta t$  and  $\beta_{initial}$  are denoted. The spatial and temporal electric and magnetic fields are discretized by Yee's algorithm. Fourier transforms of the sample points are calculated; hence the cutoff frequencies of the propagation modes can be obtained. The first cutoff frequency belongs to the first propagation mode. The propagation constant  $\beta$  can be determined by  $2\pi f/c$ , where  $f$  is the first derived cutoff frequency. After computing  $\beta$ ,  $n_{eff} = \beta/k_0$  can be obtained as a function of wavelength.

The material dispersion,  $D_m$ , is calculated by Sellmeier equation [34]:

$$n_{Silica}^2(\lambda) = \varepsilon_r(\lambda) = 1 + \sum_{k=1}^3 \frac{b_k \lambda^2}{\lambda^2 - \lambda_k^2} \quad (3)$$

where  $b_1 = 0.6961663$ ,  $b_2 = 0.4079426$ ,  $b_3 = 0.8974794$ ,  $\lambda_1 = 0.0684043 \mu\text{m}$ ,  $\lambda_2 = 0.1162414 \mu\text{m}$  and  $\lambda_3 = 9.896161 \mu\text{m}$ . The parameters  $b_k$  and  $\lambda_k$  have been obtained by fitting Eq. (3) to the experimental results of the fused silica [31].

After computing  $n_{eff}$  and  $n_{Silica}$ , as a function of  $\lambda$ , chromatic dispersion can be derived by Eq. (1). The confinement loss is another important parameter for design of PCFs which can be determined by [1]:

$$L_{conf} = 8.686 k_0 \text{Im}[n_{eff}] \text{ (dB/m)} \quad (4)$$

where  $\text{Im}$  denotes the imaginary part.

By considering irregularity in the photonic crystal fiber structure, the PCF modal birefringence can be obtained. In many applications a high birefringent photonic crystal fiber (Hi-Bi PCF) is required. In conventional PCFs, because of the shape of supercells and boundary conditions, the birefringence is low, but not zero, as can be estimated from Fig. 1. Some irregularities that can cause a high birefringence PCF are: variation of holes or rods radii, replacing the circular holes or rods with elliptical ones in the cladding and extending the defects to obtain an elliptical-shape core [8, 35–36]. Birefringence is defined as the difference between effective refractive indices of two fundamental polarization modes:

$$B(\lambda) = n_{x\text{eff}} - n_{y\text{eff}} = \frac{\lambda}{2\pi} (\beta_x(\lambda) - \beta_y(\lambda)) \quad (5)$$

where  $\beta_x$ ,  $\beta_y$  and  $n_{x\text{eff}}$ ,  $n_{y\text{eff}}$  are the propagation constants and effective refractive indices of the two orthogonal polarization modes [35].

In summary, the chromatic dispersion of the PCF has been calculated by Eq. (1). To determine the waveguide dispersion, the effective refractive index of the structure must be obtained as a function of  $\lambda/\Lambda$ , and material dispersion is computed by Eq. (3). By changing the geometry and refractive index of the PCF structure and calculating the chromatic dispersion, some types of PCFs have been designed.

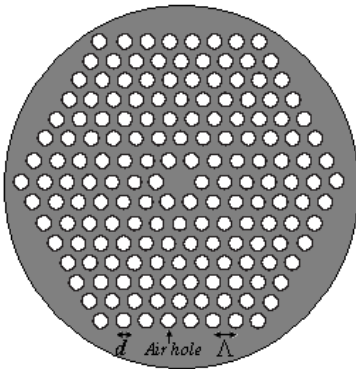


**Figure 1.** Structure of a PCF with air holes in silica in a triangular lattice around the core.

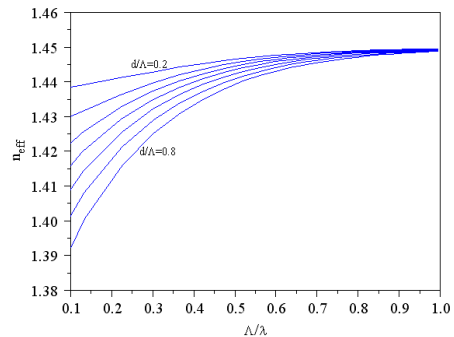


**Figure 2.** Effective refractive index of the fundamental mode  $n_{\text{eff}}$  versus  $\Lambda/\lambda$  for different holes diameters for the structures of air holes in silica of Fig. 1 with  $\Lambda = 3 \mu\text{m}$ .

Also, the confinement loss and modal birefringence of the proposed specialty fibers have been numerically derived.

### 3. DESIGN OF SPECIALTY FIBERS

Two types of photonic crystals, consisting of air holes in silica and silica rods in air have been proposed to design the specialty fibers. Refractive index of silica can be varied by different oxides, such as  $\text{GeO}_2$ ,  $\text{P}_2\text{O}_5$  and  $\text{B}_2\text{O}_3$ .

#### 3.1. PCFs Consisting of Air Holes in Silica

The fiber structures consisting of seven rows of air holes in silica with diameter  $d$  arranging a triangular lattice with a pitch of  $\Lambda$  for cladding

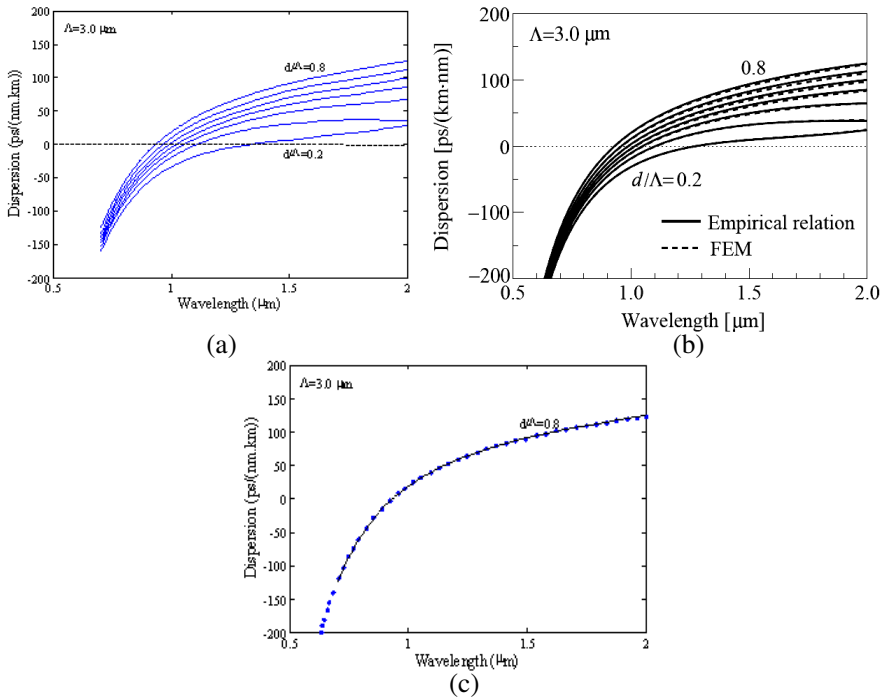


**Figure 3.** Comparison of the chromatic dispersion versus wavelength of the PCF structure of Fig. 1. (a) Derived by our software and (b) from Ref. [5], (c) exact comparison of two similar curves of (a) and (b), which shows the accuracy of our software.

have been considered, as shown in Fig. 1. In the structure, the core is silica with refractive index of 1.45 at 1550 nm.

Different parameters of these PCFs have been varied and their dispersion and loss have been computed by the methods given in Section 2. The appropriate structure has been selected from the vast number of derived results.

Figure 2 demonstrates the wavelength dependence of the effective refractive index of the fiber structure of Fig. 1 with pitch of  $\Lambda = 3 \mu\text{m}$  and diameter-pitch ratio of  $d/\Lambda$  ranging from 0.2 to 0.8. As expected, in Fig. 2 by decreasing the holes diameters,  $n_{eff}$  approaches the refractive index of the silica.

To evaluate our software, the chromatic dispersion of the photonic crystal fiber of Fig. 1 has been derived that is shown in Fig. 3(a). The results comply very well with those of reference [5], depicted in Fig. 3(b). Also, for emphasis on the validity of our software, one of the curves in Fig. 3(a) is compared to the similar one from Fig. 3(b), which is depicted in Fig. 3(c).

Material dispersion depends only on the waveguide material, but waveguide dispersion is a function of the core radius, the fiber relative refractive index difference, and the refractive index profile. Therefore, the waveguide dispersion and the chromatic dispersion can be varied with the fiber parameters design [37].

Here, we have proposed several types of specialty fibers designed by photonic crystals.

### 3.1.1. Dispersion Shifted PCF

Most of the conventional single mode fibers used in telecommunication systems and networks had minimum dispersion at 1300 nm wavelength. By varying the refractive index profile and creating a fiber with larger negative waveguide dispersion, the zero dispersion wavelength could be shifted to the longer wavelengths such as 1550 nm which is called dispersion shifted fibers (DSFs) to be used in the third telecommunication window.

In our design, by setting  $\Lambda = 2 \mu\text{m}$  and  $d/\Lambda = 0.6$  for the structure of Fig. 1, the value of chromatic dispersion is equal to 90.43 (ps/(nm·km)) at 1550 nm, but as demonstrated in Fig. 4, by replacing the first row of the air holes by a material with refractive index of 1.35, changing the shape of the first circular holes array with  $d_1 = 1.2 \mu\text{m}$  to elliptical holes with dimensions of  $1.2 \mu\text{m} \times 1.7 \mu\text{m}$ , as depicted in Fig. 5, the zero dispersion wavelength shifts to 1535 nm.

The confinement loss and the birefringence of this structure at 1550 nm are  $4.69 \times 10^{-6}$  (dB/m) and  $8.6412 \times 10^{-5}$ , respectively.

In order to evaluate the characteristics of our proposed DS-PCF, we have computed the confinement loss and the birefringence of a conventional PCF with  $\Lambda = 2 \mu\text{m}$  and  $d/\Lambda = 0.6$ , with our software, the

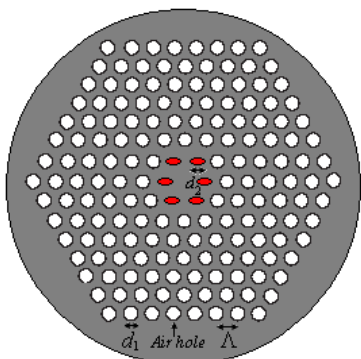


**Figure 4.** Structure of the proposed DS-PCF consisting of air holes in silica with  $\Lambda = 2 \mu\text{m}$ ,  $d_1 = 1.2 \mu\text{m}$ ,  $d_2 = 1.7 \mu\text{m}$ .

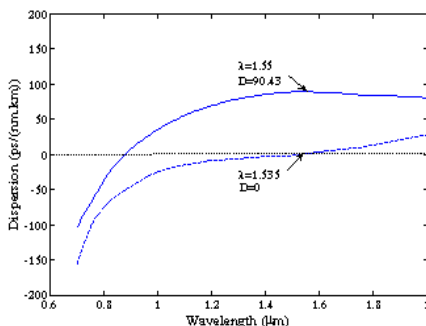


**Figure 5.** Chromatic dispersion of the DS-PCF versus wavelength. The solid line shows the dispersion of the PCF structure of Fig. 1 with  $\Lambda = 2 \mu\text{m}$  and  $d/\Lambda = 0.6$ , while the dashed line shows the dispersion for the PCF with refractive index of 1.35 for the elliptical holes at the first row with  $d_2 = 1.7 \mu\text{m}$ .

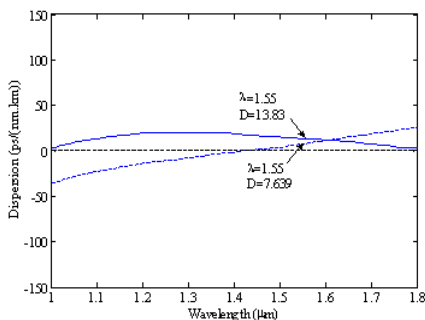


**Figure 6.** Chromatic dispersion versus wavelength for the NZ-DS-PCF structure of Fig. 1. The solid line shows the dispersion for the PCF with elliptical holes at the first row with  $\Lambda = 2 \mu\text{m}$ ,  $d_2 = 1.9 \mu\text{m}$  and refractive index of 1.3. The dashed line shows the dispersion for circular holes at the first row with  $\Lambda = 2.5 \mu\text{m}$ , refractive index of 1.4 and diameter of  $2 \mu\text{m}$ .

results of which are  $4.77 \times 10^{-2}$  (dB/m) and  $5.5578 \times 10^{-6}$ , respectively. These parameters are complied with those of reference [15]. Comparing the confinement loss and birefringence of our proposed DS-PCF with those of conventional ones show that the loss of our design is lower, but the birefringence is higher.

### 3.1.2. Non-Zero Dispersion Shifted PCF

To control the detrimental nonlinear effects of the PCFs, a small amount of dispersion at 1550 nm is required. To design these non-zero dispersion shifted fibers (NZ-DSFs), a new fiber structure of Fig. 1 with  $\Lambda = 2 \mu\text{m}$ ,  $d/\Lambda = 0.7$  and the refractive index of 1.3 for the first row of the elliptical holes with  $d_2 = 1.9 \mu\text{m}$  has been designed and proposed. As demonstrated in Fig. 6, the chromatic dispersion at 1550 nm is equal to 13.83 (ps/(nm·km)). By increasing the refractive index of the first row to 1.4, the dispersion increases to 17.07 (ps/(nm·km)) at 1550 nm.

The birefringences of these two NZ-DS-PCF are equal to  $8.2147 \times 10^{-5}$  and  $5.0646 \times 10^{-5}$  at 1550 nm, and the confinement losses at 1550 nm are  $1.37 \times 10^{-5}$  and  $1.38 \times 10^{-8}$  (dB/m), respectively. The second NZ-DS-PCF has lower imaginary part of  $n_{eff}$ , thus according to Eq. (4), its loss has decreased.

Contrary to the conventional PCF with  $\Lambda = 2 \mu\text{m}$  and  $d/\Lambda = 0.7$  that has the loss of  $5.56 \times 10^{-2}$  (dB/m), the losses of above structures are low.

**Table 1.** New designs for NZ-DS-PCF of Fig. 1.

Characteristics	NZ-DS-PCF	NZ-DS-PCF
	#1	#2
$\Lambda$ ( $\mu\text{m}$ )	2.5	2.5
$d/\Lambda$	0.2	0.2
Refractive index of the first row of the cladding holes	1.35	1.4
The value of increasing the diameter of the first row of the cladding holes ( $\mu\text{m}$ )	-	0.5
Dispersion (ps/(nm·km))	9.014	10.6
Confinement Loss at 1550 nm (dB/m)	$0.1 \times 10^{-2}$	$1.43 \times 10^{-2}$
Birefringence at 1550 nm	$3.53 \times 10^{-7}$	$3.56 \times 10^{-7}$

Another design is for a PCF with  $\Lambda = 2.5 \mu\text{m}$ ,  $d/\Lambda = 0.6$  and increasing the diameter of the first row of circular holes to  $2 \mu\text{m}$  with refractive index of 1.4. The chromatic dispersion of the NZ-DS-PCF is  $7.639 \text{ (ps/(nm}\cdot\text{km))}$  at  $1550 \text{ nm}$ , as depicted in Fig. 6. The birefringence and the confinement loss of the PCF are  $8.1 \times 10^{-8}$  and  $1.66 \times 10^{-6} \text{ (dB/m)}$ , respectively.

Additional designs for non-zero dispersion shifted fibers are listed in Table 1 for the structure of Fig. 1. Comparing the results given in Table 1 with two designs of elliptical holes at the first row of the cladding show that the chromatic dispersion and birefringence of the NZ-DS-PCFs of Table 1 is lower, whereas the confinement loss is higher. So, there is a trade-off between these parameters for choosing a suitable NZ-DS-PCF.

### 3.1.3. Negative Dispersion PCF

All the above NZ-DS-PCFs designs have a small positive dispersion at  $1550 \text{ nm}$ . Here we introduce other structures with small negative dispersion at  $1550 \text{ nm}$ . For the PCFs with  $\Lambda = 2.5 \mu\text{m}$  or  $2 \mu\text{m}$  and  $d/\Lambda = 0.2$ , the dispersions are  $-2.069$  and  $-9.513 \text{ (ps/(nm}\cdot\text{km))}$ , respectively, as depicted in Fig. 7. Due to the symmetry of the structure, they have low birefringence of  $9.88 \times 10^{-7}$  and  $1.919 \times 10^{-6}$  at  $1550 \text{ nm}$ , respectively. If for the second design, we increase  $d/\Lambda$  to  $0.8$  and reshape the circular holes to elliptical with refractive index of 1.4 in the first row, the dispersion and birefringence become  $-6.71 \text{ (ps/(nm}\cdot\text{km))}$  and  $2.5915 \times 10^{-5}$  at  $1550 \text{ nm}$ , respectively. The confinement losses of these three structures at  $1550 \text{ nm}$  wavelength are

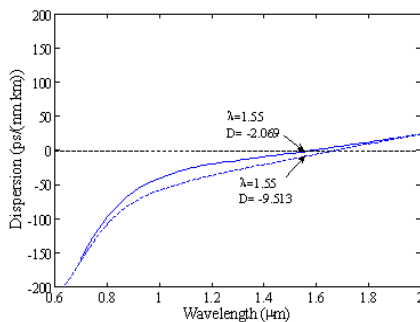


**Figure 7.** Negative chromatic dispersion of NZ-DS-PCF versus wavelength for the PCF structure of Fig. 1 with  $d/\Lambda = 0.2$ ,  $\Lambda = 2.5 \mu\text{m}$  (solid line) and  $\Lambda = 2 \mu\text{m}$  (dashed line).

$2.12 \times 10^{-2}$ ,  $1.99 \times 10^{-2}$  and  $3.05 \times 10^{-7}$  (dB/m), respectively. The confinement loss of the third design which obtained by some variation of the second PCF is much less than that of the conventional PCF with  $\Lambda = 2 \mu\text{m}$  and  $d/\Lambda = 0.8$ . Hence, there is a trade-off between the ease of fabrication, chromatic dispersion and confinement loss.

#### 3.1.4. Dispersion Flattened PCF

The chromatic dispersion of the dispersion flattened photonic crystal fibers (DF-PCFs) must regularly be flattened in the range of 1.3–1.6  $\mu\text{m}$ . In our simulation for Fig. 1, by choosing  $\Lambda = 2 \mu\text{m}$ ,  $d_{1o} = 0.8 \mu\text{m}$  and decreasing the diameter of the first holes to  $d_{1i} = 0.7 \mu\text{m}$  (Fig. 8) the PCF has a flat dispersion between 1380 and 1600 nm with a maximum variation of 0.74 (ps/(nm·km)), as shown in Fig. 9.

By increasing the diameter-pitch ratio to  $d/\Lambda = 0.6$ , changing the circular holes to elliptical at the first row of the structure with  $d_2 = 1.7 \mu\text{m}$  and refractive index of 1.3, the DF-PCF has a dispersion about 8.8 (ps/(nm·km)) over the range of 1450 to 1600 nm.

By choosing  $d/\Lambda = 0.7$ , refractive index of the first elliptical hole row of 1.35 and  $d_2 = 1.9 \mu\text{m}$ , the DF-PCF has the nearly zero negative dispersion over the range of 1300 to 1560 nm, as demonstrated in Fig. 10. The confinement losses of these four structures are  $3.44 \times 10^{-5}$ ,  $6.52 \times 10^{-6}$ ,  $9.01 \times 10^{-8}$  (dB/m) and their modal birefringences are

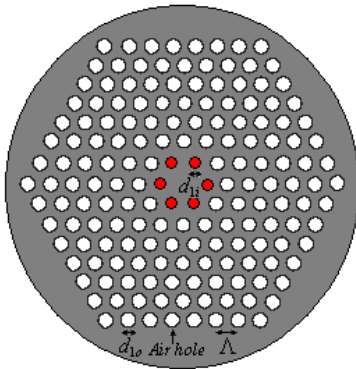


**Figure 8.** Structure of the proposed DF-PCF consisting of air holes in silica with  $\Lambda = 2 \mu\text{m}$ ,  $d_{1o} = 0.8 \mu\text{m}$ , and  $d_{1i} = 0.7 \mu\text{m}$ .

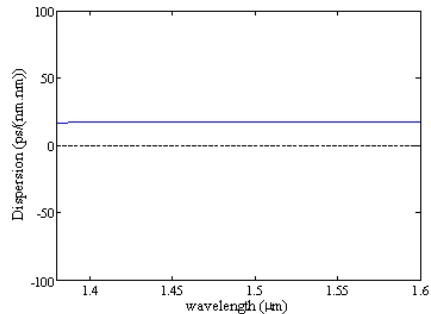


**Figure 9.** Chromatic dispersion of the DF-PCF structure of Fig. 8 versus wavelength with  $\Lambda = 2 \mu\text{m}$  and  $d/\Lambda = 0.4$ . The diameters of the holes at the first row are reduced to  $0.7 \mu\text{m}$ .

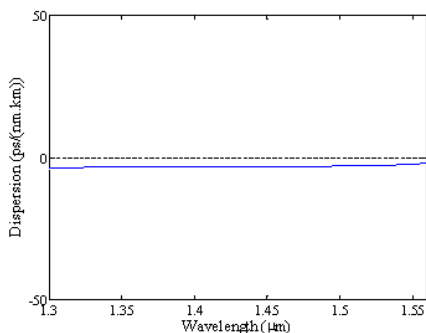


**Figure 10.** The negative chromatic dispersion of DF-PCF structure of Fig. 1 versus wavelength with  $\Lambda = 2 \mu\text{m}$ ,  $d/\Lambda = 0.7$ , refractive index of the first elliptical holes row of 1.35 and  $d_2 = 1.9 \mu\text{m}$ .

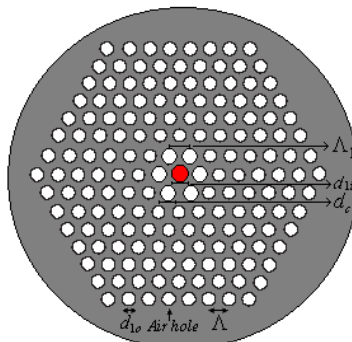


**Figure 11.** Structure of the proposed DC-PCF with air holes in silica,  $\Lambda = 1 \mu\text{m}$ ,  $\Lambda_1 = 0.8 \mu\text{m}$ ,  $d_{1o} = 0.6 \mu\text{m}$ ,  $d_{1i} = 0.7 \mu\text{m}$  and  $d_c = 0.8 \mu\text{m}$ .

$1.169 \times 10^{-6}$ ,  $1.0755 \times 10^{-4}$  and  $7.2507 \times 10^{-5}$ , respectively, at 1550 nm wavelength. The confinement losses of these DF-PCF are much less than the conventional PCF with  $\Lambda = 2 \mu\text{m}$  and  $d/\Lambda = 0.4$  that has the loss of  $4.1 \times 10^{-3}$  (dB/m).

### 3.1.5. Dispersion Compensating PCF

In order to increase the capacities of the long haul optical communication systems and networks, WDM systems have been designed. In single wavelength and WDM systems, fiber must have appropriate dispersion to control the detrimental nonlinear effects, such as self phase modulation (SPM), cross phase modulation (XPM) and four wave mixing (FWM). One approach for reducing the nonlinear effects of SPM, XPM and FWM in WDM systems is to use conventional single mode fibers for the transmission media and compensating the dispersion by using dispersion compensating fibers (DCFs) in appropriate distances. Dispersion compensating fibers have a large negative dispersion to compensate the main fiber dispersion. Conventional dispersion compensating fibers do not have high negative chromatic dispersion, while by using photonic crystal fibers, it is possible to design DCFs with higher negative dispersion around 1550 nm.

The first designed structure of the DC-PCF is demonstrated in

Fig. 11, with  $\Lambda = 1 \mu\text{m}$ ,  $\Lambda_1 = 0.8 \mu\text{m}$  and  $d/\Lambda = 0.6$ . The diameter of the first row of circular holes, core diameter and the refractive index of the core are  $d_{1i} = 0.7 \mu\text{m}$ ,  $d_c = 0.8 \mu\text{m}$  and 1.52, respectively. The DC-PCF has dispersion of  $-1270$  (ps/(nm·km)) at 1550 nm, as depicted in Fig. 12(a).

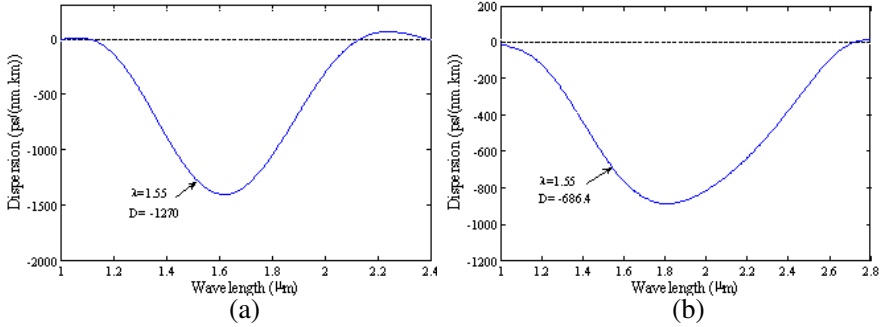


**Figure 12.** Chromatic dispersion of the DC-PCF with air holes in silica versus wavelength for  $\Lambda = 1 \mu\text{m}$ ,  $\Lambda_1 = 0.8 \mu\text{m}$ , refractive index of the core is 1.52,  $d_{1o} = 0.6 \mu\text{m}$ ,  $d_{1i} = 0.7 \mu\text{m}$ ,  $d_c = 0.8 \mu\text{m}$ , (a)  $d/\Lambda = 0.6$  and (b)  $d/\Lambda = 0.7$ .

**Table 2.** New designs for DC-PCF of Fig. 1.

Characteristics	DC-PCF #1	DC-PCF #2
$\Lambda$ ( $\mu\text{m}$ )	1	1
$\Lambda_1$ ( $\mu\text{m}$ )	0.8	0.8
$d/\Lambda$	0.6	0.6
Diameter of the first row of the cladding holes ( $\mu\text{m}$ )	0.7	0.7
Diameter of the core ( $\mu\text{m}$ )	0.8	0.8
Refractive index of the core	1.53	1.55
Dispersion (ps/(nm·km))	-1262	-1179
Confinement Loss at 1550 nm (dB/m)	$3.01 \times 10^{-4}$	$5.09 \times 10^{-5}$
Birefringence at 1550 nm	$2.03 \times 10^{-4}$	$3.54 \times 10^{-4}$

The birefringence and confinement loss of this structure are  $1.137 \times 10^{-4}$  and  $1.9 \times 10^{-3}$  (dB/m) at 1550 nm, respectively. By increasing the refractive index of the core, the chromatic dispersion and the confinement loss decrease. The results are summarized in

Table 2.

The second design is similar to the first one, but without increasing the diameter of the first row of the circular holes and core. In this case, the chromatic dispersion decreases, but the confinement loss of the structure diminishes by an order of magnitude. By setting  $\Lambda = 1 \mu\text{m}$ ,  $\Lambda_1 = 0.8 \mu\text{m}$ ,  $d/\Lambda = 0.7$  and  $n_{co} = 1.52$ , the chromatic dispersion is equal to  $-686.4 \text{ (ps/(nm}\cdot\text{km))}$  at 1550 nm, as depicted in Fig. 12(b). The birefringence and confinement loss of this structure are  $4.3728 \times 10^{-5}$  and  $1.29 \times 10^{-6} \text{ (dB/m)}$  at 1550 nm, respectively. The birefringence and loss of this structure are much lower than those of the first design. The losses have increased when  $\Lambda$  decreased [17], while the losses of the conventional PCFs are much higher than these proposed structures.

3.1.6. Polarization Maintaining PCF

Polarization maintaining fibers (PMFs) have an important role in fiber-based measurements and transmission systems. By using PMFs the polarization of lightwave launched into the fiber remains constant during propagation. Also, they can eliminate the effect of polarization mode dispersion (PMD). Polarization maintaining photonic crystal fibers (PM-PCFs) have an asymmetric structure along two orthogonal axes which leads to a high effective refractive index difference between two orthogonal polarization modes and high birefringence.

We have introduced an asymmetric structure with high birefringence, as shown in Fig. 13 to be utilized as PM-PCF. By setting  $\Lambda = 1 \mu\text{m}$ ,  $\Lambda_1 = 0.8 \mu\text{m}$ ,  $\Lambda_2 = 0.7 \mu\text{m}$ ,  $d/\Lambda = 0.6$  and refractive index of 1.52 for the core, the PCF shows high birefringence

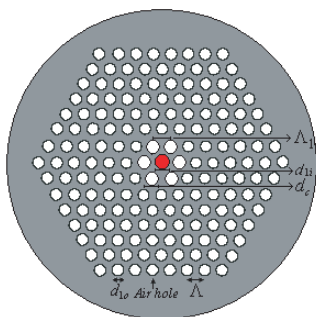


Figure 13. Structure of the proposed PMF-PCF with air holes in silica,  $\Lambda = 1 \mu\text{m}$ ,  $\Lambda_1 = 0.8 \mu\text{m}$ ,  $\Lambda_2 = 0.7 \mu\text{m}$  and  $d/\Lambda = 0.6$ .

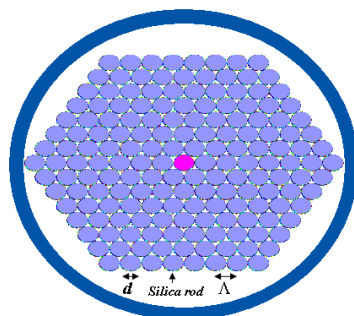


Figure 14. Structure of a PCF consisting of silica rods in air in a triangular lattice around the core.

of  $2.5 \times 10^{-3}$ . The PMF-PCF has chromatic dispersion and confinement loss of  $-767.6$  (ps/(nm·km)) and  $1.5 \times 10^{-3}$  (dB/m) at 1550 nm, respectively. By increasing the refractive index of the core to 1.55, the PMF-PCF birefringence increases to  $3 \times 10^{-3}$ , and its chromatic dispersion and confinement loss changes to  $-949.7$  (ps/(nm·km)) and  $3.37 \times 10^{-4}$  (dB/m) at 1550 nm, respectively.

### 3.2. PCFs Consisting of Silica Rods in Air

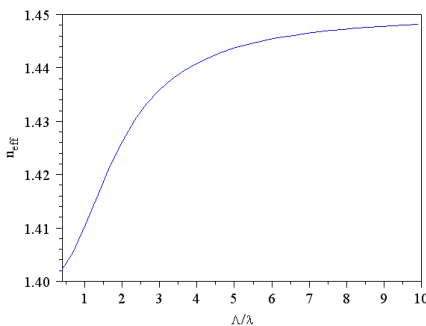
It is possible to introduce some fibers designed by PCF consisting of silica rods in air. This type of PCF can be fabricated by rod-in-tube method by high index rods in a medium of lower refractive index inside a tube [38]. Here, the silica rods with refractive index of 1.45 and diameter-pitch ratio of  $d/\Lambda = 1$  are located in air, as shown in Fig. 14. The amount of core lightwave that penetrate the sixth row of rods is very low and can be neglected. Therefore, for ease and similarity of the simulations, some rods inside the surrounding tube are removed to create similarity between Figs. 1 and 14.

Figure 15 demonstrates the wavelength dependence of the effective refractive index of the fiber structure of Fig. 14 with pitch of  $\Lambda = 3 \mu\text{m}$  and  $d/\Lambda = 1$ , which is required for waveguide dispersion calculations.

With the above structure, some specialty fibers can be designed.

#### 3.2.1. Negative Dispersion PCF

The structure for the negative NZ-DS-PCF with silica rods in air has  $\Lambda = 3 \mu\text{m}$  and the core refractive index of 1.48. The chromatic



**Figure 15.** Effective refractive index of the fundamental mode  $n_{eff}$  versus  $\Lambda/\lambda$  for the structure of Fig. 14 with  $\Lambda = 3$  and  $d/\Lambda = 1$ .

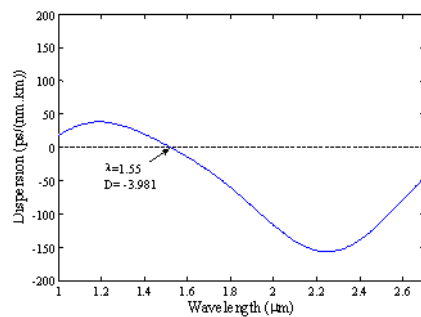


**Figure 16.** Negative chromatic dispersion of the NZ-DS-PCF versus wavelength of the PCF structure of Fig. 14 with  $\Lambda = 3 \mu\text{m}$ .

dispersion becomes  $-3.981$  (ps/(nm·km)) at 1550 nm, as shown in Fig. 16.

The confinement loss and the birefringence of this structure at 1550 nm are  $3.18 \times 10^{-2}$  (dB/m) and  $2.46 \times 10^{-6}$ , respectively. Contrary to the NZ-DS-PCF consisting of air holes in silica described in Section 3.1.3, we have designed the negative dispersion PCF without replacing the circular rods of the first row by elliptical ones, but the loss of this NZ-DS-PCF is higher.

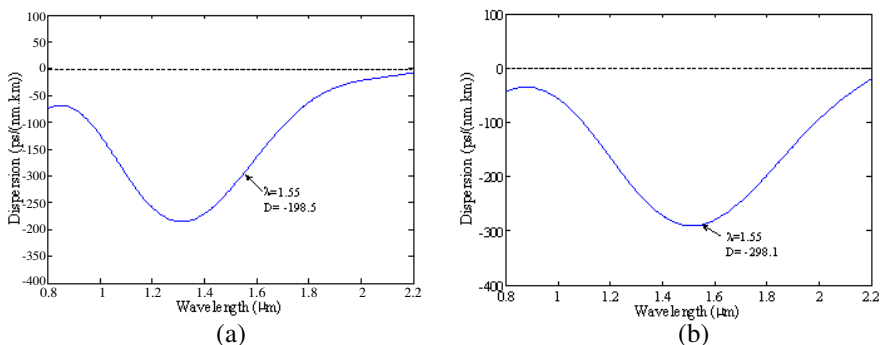


**Figure 17.** Chromatic dispersion of the DC-PCF with silica rods in air versus wavelength for  $\Lambda = 2 \mu\text{m}$ . Refractive index of the core is 1.47 (a) and 1.48 (b).

**Table 3.** New designs for DC-PCF of Fig. 14.

Characteristics	NZ-DS-PCF	NZ-DS-PCF
	#1	#2
$\Lambda$ ( $\mu\text{m}$ )	2	2
$d/\Lambda$	1	1
Refractive index of the core	1.49	1.5
Refractive index of the first row of the cladding rods	1.45	1.45
Dispersion (ps/(nm·km))	-270.8	-224.7
Confinement Loss at 1550 nm (dB/m)	0.11	0.1066
Birefringence at 1550 nm	$5.32 \times 10^{-6}$	$5.16 \times 10^{-6}$

### 3.2.2. Dispersion Compensating PCF

The first DC-PCF with silica rods in air has been designed by setting  $\Lambda = 2\ \mu\text{m}$  and refractive index of the core to 1.47. As shown in Fig. 17, the chromatic dispersion of the DC-PCF is equal to  $-198.5$  (ps/(nm·km)). By increasing the refractive index of the core to 1.48, the dispersion becomes  $-298.1$  (ps/(nm·km)). The confinement loss and the birefringence of these two structures at 1550 nm are  $9.62 \times 10^{-2}$ ,  $10.35 \times 10^{-2}$  (dB/m),  $5.34 \times 10^{-6}$  and  $5.47 \times 10^{-6}$ , respectively. Other designs are listed in Table 3. As illustrated in Table 3, by decreasing the refractive index of the core the chromatic dispersion increases.

Contrary to the structure of Fig. 11, the desirable result has been obtained for the PCF of Fig. 14, without shifting the first row of rods towards core, but the confinement losses of these structures have increased.

## 4. CONCLUSION

In this paper, by reshaping the cladding holes, varying the holes diameters in one or two rows around the core or changing the refractive index of the rods or the holes, different kinds of specialty photonic crystal fibers, such as dispersion shifted fibers (DSFs), non-zero DSFs (NZ-DSFs), dispersion flattened fibers (DFFs), dispersion compensating fibers (DCFs) and polarization maintaining fibers (PMFs), have been designed and proposed. Two types of structures, air holes in silica and silica rods in air in a triangular lattice around the core have been proposed. All the proposals are for the third communication window, therefore, for both structures the core is silica and the light propagates in the PCF by total internal reflection. The chromatic dispersion, confinement loss and modal birefringence of the proposed specialty fibers have been numerically derived. The confinement losses of the proposed structures are lower than those of the conventional PCFs. Moreover, contrary to the PCF with air holes in silica, for the PCF consisting of silica rods in air, NZ-DS-PCF and DC-PCF have been designed without replacing the circular rods of the first row by elliptical ones or shifting the first row of rods towards core, but the confinement losses of these structures have increased. Therefore, there is a trade-off between the confinement loss and the ease of fabrication of the structure.

## REFERENCES

1. Saitoh, K., M. Koshiba, T. Hasegawa, and E. Sasaoka, "Chromatic dispersion control in photonic crystal fibers: Application to ultra-flattened dispersion," *Opt. Express*, Vol. 11, 843–852, 2003.
2. Saitoh, K. and M. Koshiba, "Numerical modeling of photonic crystal fibers," *IEEE J. Lightwave Technol.*, Vol. 23, 3580–3590, 2005.
3. Pourkazemi, A. and M. Mansourabadi, "Comparison of fundamental space-filling mode index, effective index and the second and third order dispersion of photonic crystal fibers calculated by scalar effective index method and empirical relations methods," *Progress In Electromagnetics Research M*, Vol. 1, 197–206, 2008.
4. Lægsgaard, J., A. Bjarklev, and S. E. B. Libori, "Chromatic dispersion in photonic crystal fibers fast and accurate scheme for calculation," *J. Opt. Soc. Am. B*, Vol. 20, 443–448, 2003.
5. Saitoh, K. and M. Koshiba, "Empirical relations for simple design of photonic crystal fibers," *Opt. Express*, Vol. 13, 267–274, 2004.
6. Uranus, H. P., H. J. W. M. Hoekstra, and E. Van Groesen, "Modes of an endlessly single-mode photonic crystal fiber: A finite element investigation," *Proc. 11th IEEE Symp. Commun. and Vehicular Technol. (SCVT)*, Ghent University, Gent, Belgium, 2004.
7. Poli, F., M. Foroni, M. Bottacini, M. Fuochi, N. Burani, L. Rosa, A. Cucinotta, and S. Selleri, "Single-mode regime of square-lattice photonic crystal fibers," *J. Opt. Soc. Am. B*, Vol. 22, 1655–1661, 2005.
8. Antkowiak, M., R. Kotynski, T. Nasilowski, P. Lesiak, J. Wojcik, W. Urbanczyk, F. Berghmans, and H. Thienpont, "Phase and group modal birefringence of triple-defect photonic crystal fibers," *J. Opt. A: Pure Appl. Opt.*, Vol. 7, 763–766, 2005.
9. Wang, J., C. Jiang, W. Hu, and M. Gao, "Properties of index-guided PCF with air-core," *Optics and Laser Technol.*, Vol. 39, 317–321, 2007.
10. Chen, D. and L. Shen, "Ultrahigh birefringent photonic crystal fiber with ultralow confinement loss," *IEEE J. Photon. Technol. Lett.*, Vol. 19, 185–187, 2007.
11. Yang, T. J., L. F. Shen, Y. F. Chau, M. J. Sung, D. Chen, and D. P. Tsai, "High birefringence and low loss circular air-holes photonic crystal fiber using complex unit cells in cladding," *Opt. Commun.*, Vol. 281, 4334–4338, 2008.
12. Hai, N. H., Y. Namihir, F. Begum, S. F. Kaijage, T. Kinjo, S. M. A. Razzak, and N. Zou, "A novel photonic crystal fiber

- design for large effective area and high negative dispersion,” *IEICE Trans. Electron.*, Vol. E91-C, 113–116, 2008.
13. Guenneau, S., A. Nicolet, F. Zolla, and S. Lasquelec, “Numerical and theoretical study of photonic crystal fibers,” *Progress In Electromagnetics Research*, PIER 41, 271–305, 2003.
  14. Wu, J.-J., D. Chen, K.-L. Liao, T.-J. Yang, and W.-L. Ouyang, “The optical properties of Bragg fiber with a fiber core of 2-dimension elliptical-hole photonic crystal structure,” *Progress In Electromagnetics Research Letters*, Vol. 10, 87–95, 2009.
  15. Haxha, S. and H. Ademgil, “Novel design of photonic crystal fibers with low confinement losses, nearly zero ultra-flatted chromatic dispersion, negative chromatic dispersion and improved effective mode area,” *Opt. Commun.*, Vol. 281, 278–286, 2008.
  16. Chen, M. and S. Xie, “New nonlinear and dispersion flattened photonic crystal fiber with low confinement loss,” *Opt. Commun.*, Vol. 281, 2073–2076, 2008.
  17. Chiang, J. S. and T. L. Wu, “Analysis of propagation characteristics for an octagonal photonic crystal fiber (O-PCF),” *Opt. Commun.*, Vol. 258, 170–176, 2006.
  18. Musin, R. R. and A. M. Zheltikov, “Designing dispersion-compensating photonic-crystal fibers using a genetic algorithm,” *Opt. Commun.*, Vol. 281, 567–572, 2008.
  19. Kim, S., C. S. Kee, D. K. Ko, J. Lee, and K. Oh, “A dual-concentric-core photonic crystal fiber for broadband dispersion compensation,” *J. Korean Phys. Soc.*, Vol. 49, 1434–1437, 2006.
  20. Cho, M., J. Kim, H. Park, Y. Han, K. Moon, E. Jung, and H. Han, “Highly birefringent terahertz polarization maintaining plastic photonic crystal fibers,” *Opt. Express*, Vol. 16, 7–12, 2008.
  21. Suzuki, K., H. Kubota, S. Kawanishi, M. Tanaka, and M. Fujita, “Optical properties of a low-loss polarization-maintaining photonic crystal fiber,” *Opt. Express*, Vol. 9, 676–680, 2001.
  22. Ortigosa-Blanch, A., A. Diez, M. Delgado-Pinar, J. L. Cruz, and M. V. Andres, “Temperature independence of birefringence and group velocity dispersion in photonic crystal fibers,” *Electron. Lett.*, Vol. 40, 1327–1329, 2004.
  23. Song, W., Y. Zhao, Y. Bao, S. Li, Z. Zhang, and T. Xu, “Numerical simulation and analysis on mode property of photonic crystal fiber with high birefringence by fast multipole method,” *PIERS Online*, Vol. 3, No. 6, 836–841, 2007.
  24. Wang, L. and D. X. Yang, “A new design for terahertz photonic

- crystal fiber using the finite-difference time-domain method," *PIERS Online*, Vol. 1, No. 2, 133–136, 2005.
25. Wu, J.-J., T.-J. Yang, K.-L. Liao, D. Chen, and L. F. Shen, "Highly birefringent Bragg fiber with a fiber core of 2-dimension elliptical-hole photonic crystal structure," *PIERS Proceedings*, 185–188, Beijing, China, Mar. 23–27, 2009.
  26. Chu, S. T. and S. K. Chaudhuri, "Finite-difference time-domain method for optical waveguide analysis," *Progress In Electromagnetics Research*, PIER 11, 255–300, 1995.
  27. Kashani, Z. G., N. Hojjat, and M. Shahabadi, "Full-wave analysis of coupled waveguides in a two-dimensional photonic crystal," *Progress In Electromagnetics Research*, PIER 49, 291–307, 2004.
  28. Manzanares-Martínez, J. and J. Gaspar-Armenta, "Direct integration of the constitutive relations for modeling dispersive metamaterials using the finite difference time-domain technique," *Journal of Electromagnetic Waves and Applications*, Vol. 21, No. 15, 2297–2310, 2007.
  29. Zheng, G., A. A. Kishk, A. W. Glisson, and A. B. Yakovlev, "Implementation of Mur's absorbing boundaries with periodic structures to speed up the design process using finite-difference time-domain method," *Progress In Electromagnetics Research*, PIER 58, 101–114, 2006.
  30. El-Mashade, M. B. and M. N. Abdel Aleem, "Analysis of ultrashort pulse propagation in nonlinear optical fiber," *Progress In Electromagnetics Research B*, Vol. 12, 219–241, 2009.
  31. Sha, W. E. I., X.-L. Wu, Z.-X. Huang, and M.-S. Chen, "Waveguide simulation using the high-order symplectic finite-difference time-domain scheme," *Progress In Electromagnetics Research B*, Vol. 13, 237–256, 2009.
  32. Wei, B., S.-Q. Zhang, Y.-H. Dong, and F. Wang, "A general FDTD algorithm handling thin dispersive layer," *Progress In Electromagnetics Research B*, Vol. 18, 243–257, 2009.
  33. Taflov, A. and S. C. Hagness, *Computational Electrodynamics: The Finite-difference Time-domain Method*, 3rd edition, Artech House, Boston, 2005.
  34. Agrawal, G. P., *Nonlinear Fiber Optics*, 4th edition, Academic Press, Boston, 2007.
  35. Li, S., Y. Li, Y. Zhao, G. Zhou, Y. Han, and L. Hou, "Correlation between the birefringence and the structural parameter in photonic crystal fiber," *Opt. and Laser Technol.*, Vol. 40, 663–667, 2008.

36. Hwang, I. K., Y. J. Lee, and Y. H. Lee, "Birefringence induced by irregular structure in photonic crystal fiber," *Opt. Express*, Vol. 11, 2799–2806, 2003.
37. Keiser, G., *Optical Fiber Communications*, 3rd edition, McGraw-Hill, New York, 2000.
38. Seraji, F. E., M. Rashidi, and M. Karimi, "Characteristics of holey fibers fabricated at different drawing speeds," *Chinese Opt. Lett.*, Vol. 5, 131–134, 2007.